The orientation of the crystal with respect to rotation around the scattering vector was the same for all scans at a particular ν value. The mean path lengths through the crystal are therefore the same for all these scans. This was not the case for the scans at different ν, hence the difference between the average F^2 at the two ν positions.

We thank Claude Zeyen and Mogens Lehmann for constructive discussions.

References

AXE, J. D. & HASTINGS, J. B. (1983). *Acta Cryst.* A**39**, 593-594.

AZAROFF, L. V. (1968). *Elements of X-ray Crystallography.* New York: McGraw-Hill.

BUSING, W. R. & LEVY, H. A. (1967). *Acta Cryst.* **22**, 457-464.

LEBECH, B. & NIELSEN, M. (1975). *New Methods and Techniques in Neutron Diffraction.* Report RCN-234, pp. 466-486. Petten: Reactor Centrum Nederland.

LEHMANN, M. S. (1975). *J. Appl. Cryst.* **8**, 619-622.

LIPSON, H. (1972). *International Tables for X-ray Crystallography*, Vol. II, Section 5.2.5. Birmingham: Kynoch Press. (Present distributor D. Reidel, Dordrecht.)

PRINCE, E., WLODAWER, A. & SANTORO, A. (1978). *J. Appl. Cryst.* **11**, 173-178.

THOMAS, M., STANSFIELD, R. F. D., BERNERON, M., FILHOL, A., GREENWOOD, G., JACOBÉ, J., FELTIN, D. & MASON, S. A. (1983). *Position-Sensitive Detection of Thermal Neutrons*, edited by P. CONVERT & J. B. FORSYTH, pp. 344-350. New York: Academic Press.

Acta Cryst. (1988). A**44**, 262-270

On the Statistical Dynamical Theory of Diffraction: Application to Silicon

BY M. AL HADDAD* AND P. J. BECKER

Laboratoire de Cristallographie, CNRS and Université Scientifique et Médicale de Grenoble, 166X, 38042 Grenoble CEDEX, France

(*Received* 15 *September* 1987; *accepted* 23 *November* 1987)

Abstract

A detailed solution of Kato's equations describing the propagation of X-rays or neutrons in a crystal containing a statistical distribution of imperfections is presented: this solution makes use of propagation operators to describe multiple scattering events. Corrections to Kato's original solution are given which have a significant effect, even in the case of crystals with a high degree of long-range perfection. The present modified solution is applied to experimental measurement on parallel plates of silicon with different dislocation densities by Olekhnovich, Karpei, Olekhnovich & Puzenkova [*Acta Cryst.* (1983), A**39**, 116-122]. The theory reproduces observations quite well, in contrast to conclusions reached by Olekhnovich *et al.* on the basis of the original solution. It can be inferred that the basic ideas of Kato allow for a correct interpretation of diffraction reflectivities in highly perfect crystals, where a significant contribution from incoherent components of scattered intensities must be incorporated. However, the theory has to be modified for the case of lower long-range perfection: this involves the modification of the expressions for the effective correlation lengths that enter the theory.

I. Introduction

Until 1980, extinction was treated by two very different approaches. Following the ideas of Darwin (1914, 1922), the mosaic model was introduced. In such a model, one considers perfectly coherent multiple scattering within perfect mosaic block, the so-called *primary extinction*, and totally incoherent multiple scattering between adjacent blocks, the so-called *secondary extinction.*

Secondary extinction is therefore described by *energy coupling* equations between the incident and diffracted beams (Zachariasen, 1967; Becker & Coppens, 1974; Kato, 1976), the solution of which is difficult due to the boundary conditions imposed by the sample. Primary extinction, on the other hand, is commonly dealt with through the *amplitude coupling* equations of dynamical theory (Zachariasen, 1945; Batterman & Cole, 1964; Authier, 1970) for perfect crystals.

Mosaic theory is quite popular in crystallography, and has been successfully applied to many practical situations, according in particular to the solution of Becker & Coppens (1974, 1975). Despite this success, it is physically doubtful, since it separates various regions of space discontinuously and arbitrarily. It is clear that distortions from perfect periodicity are much more subtle. A correct model should contain as extreme limits perfect-crystal and mosaic-crystal

* Permanent address: Atomic Energy Commission, PO Box 6091, Damascus, Syria.

0108-7673/88/030262-09$03.00

theories, and should fill the gap between those two extremes.

The gap between pure dynamical and mosaic-crystal theories has been filled by Kato (1980*a*, *b*), hereafter denoted by K*a*, *b*, in a series of two papers in which crystal imperfections are treated on a statistical basis. This theory is based on Takagi-Taupin equations for wave propagation in an imperfect crystal (see, for example, Takagi, 1969; Kato, 1973):

$$\begin{aligned}\partial D_0/\partial s_0 &= i\kappa_{-h}\varphi(s_0, s_h)D_h(s_0, s_h)\\ \partial D_h/\partial s_h &= i\kappa_h\varphi^*(s_0, s_h)D_0(s_0, s_h),\end{aligned} \tag{1}$$

where D_0 and D_h are the amplitudes of the incident and scattered waves respectively,

$$\kappa_h = (\lambda aC/V)F_h. \tag{2}$$

λ is the wavelength, C the polarization factor, V the unit-cell volume, a is 10^{-14} m for neutrons and $0{\cdot}28\times 10^{-14}$ m for X-rays. F_h is the structure factor and s_0 and s_h are the coordinates along the incident- and scattered-beam directions. The phase term φ depends on the local distortion $\mathbf{u}(\mathbf{r})$ as

$$\varphi(s_0, s_h) = \exp(2\pi i\mathbf{h}\,.\,\mathbf{u}), \tag{3}$$

where $\mathbf{h}$ is the reciprocal-lattice vector.

One may write

$$\kappa_h = \kappa_h' + i\kappa_h'', \qquad \Lambda = 1/|\kappa_h'|,$$

where κ_h'' is the imaginary anomalous part, and Λ the extinction length.

Kato introduces two order parameters E and τ:

$$E = \langle\varphi(s_0, s_h)\rangle \tag{4}$$

is a long-range-order parameter, which plays the role of a static Debye-Waller factor. $\langle\ldots\rangle$ means an ensemble average over a small volume. τ, the short-range-order parameter, is a measure of the phase fluctuations, and is defined as follows. We write

$$\varphi = \langle\varphi\rangle + \delta\varphi = E + \delta\varphi.$$

The autocorrelation function of the phase φ is

$$\begin{aligned}\langle\varphi^*(s_0 - z, s_h)\varphi(s_0, s_h)\rangle &= \langle\varphi^*(s_0, s_h - z)\varphi(s_0, s_h)\rangle\\ &= E^2 + (1 - E^2)g(z).\end{aligned}$$

$g(z)$ is the intrinsic correlation function, with $g(0) = 1$. It is assumed to be real and symmetric in z and to decay rapidly.

$$\tau = \int_0^\infty g(z)\,\mathrm{d}z \tag{5}$$

is the correlation length of the phase fluctuations, the distance above which the phase correlation is lost. τ_n, the nth-order correlation length, is defined by

$$\tau_n = \int_0^\infty [g(z)]^n\,\mathrm{d}z$$

with

$$\tau_n < \tau_{n-1} < \ldots < \tau_2 < \tau.$$

Higher-order correlation functions can be defined, but at the present stage of theory one only takes into consideration pair correlations. More advanced treatments seem to be at present intractable.

Taking into consideration only pair correlations, Kato obtains two sets of propagation equations.

(1) The coherent part of the intensities is

$$I_0^c = |\langle D_0\rangle|^2, \qquad I_h^c = |\langle D_h\rangle|^2,$$

where the coherent waves $\langle D_0\rangle$ and $\langle D_h\rangle$ satisfy the following propagation equations:

$$\begin{aligned}\partial\langle D_0\rangle/\partial s_0 &= -\tfrac{1}{2}\mu_e\langle D_0\rangle + i\kappa_{-h}E\langle D_h\rangle\\ \partial\langle D_h\rangle/\partial s_h &= -\tfrac{1}{2}\mu_e\langle D_h\rangle + i\kappa_h E\langle D_0\rangle.\end{aligned} \tag{6}$$

The effective absorption coefficient μ_e is given by

$$\mu_e = \mu_0 + 2\,\mathrm{Re}\,(\kappa^2)(1 - E^2)\tau, \tag{7}$$

μ_0 is the usual absorption coefficient and $\kappa^2 = \kappa_h\kappa_{-h}$.

(2) The intensities of the incoherent beams are defined as follows:

$$\begin{aligned}I_0^i &= \langle|D_0|^2\rangle - |\langle D_0\rangle|^2 = I_0 - I_0^c\\ I_h^i &= \langle|D_h|^2\rangle - |\langle D_h\rangle|^2 = I_h - I_h^c\end{aligned} \tag{8}$$

and satisfy the propagation equations:

$$\begin{aligned}\partial I_0^i/\partial s_0 &= -\tilde{\mu}_e I_0^i + \tilde{\sigma}_{-h}I_h^i + \sigma_{-h}(1 - E^2)I_h^c\\ \partial I_h^i/\partial s_h &= -\tilde{\mu}_e I_h^i + \tilde{\sigma}_h I_0^i + \sigma_h(1 - E^2)I_0^c.\end{aligned} \tag{9}$$

In equations (9), the symbols have the following meaning:

$$\tilde{\mu}_e = \mu_0 + 2\,\mathrm{Re}\,(\kappa^2)\tau_e \tag{10}$$

is the effective absorption for incoherent beams, τ_e being the effective correlation length of the phases: if Γ is the correlation length for the fluctuations of the beams:

$$\delta D_h = D_h - \langle D_h\rangle, \qquad \delta D_0 = D_0 - \langle D_0\rangle \tag{11}$$

$$\begin{aligned}\Gamma I_h^i &= \int_0^{s_0}\langle\delta D_h^*(s_0 - z, s_h)\delta D_h(s_0, s_h)\rangle\,\mathrm{d}z\\ \tau_e &= (1 - E^2)\tau + E^2\Gamma\end{aligned} \tag{12}$$

and Kato takes for Γ the value Λ/E.

The coupling constants that appear in (9) are defined as follows:

$$\begin{aligned}\tilde{\sigma}_h &= 2|\kappa_h|^2\tau_e, \qquad \tilde{\sigma}_{-h} = 2|\kappa_{-h}|^2\tau_e,\\ \sigma_h &= 2|\kappa_h|^2\tau, \qquad \sigma_{-h} = 2|\kappa_{-h}|^2\tau,\\ \tilde{\sigma}^2 &= \tilde{\sigma}_h\tilde{\sigma}_{-h}, \qquad \sigma^2 = \sigma_h\sigma_{-h}.\end{aligned} \tag{13}$$

These six symbols are different in the presence of anomalous scattering. If this can be neglected, only two quantities remain: σ and $\tilde{\sigma}$.

The incoherent part of the intensities measures the fluctuations of the beams around their average amplitude.

Equations (6) and (9) are not mutually independent; the coherent intensities I_0^c and I_h^c are effective sources for the incoherent processes described by (9). Though some modifications to the original Kato theory will be necessary in the future, it contains a crucial idea: the fact that incoherence occurs from the coherent beam due to the local imperfections. In this paper, the validity of (6) and (9) will not be questioned.

Kato's theory has been applied to silicon crystals of various dislocation densities (Olekhnovich *et al.*, 1983). These authors conclude that even for samples of high perfection the theory is inadequate. As the Becker-Coppens approach does not work either, Olekhnovich *et al.* conclude that no available theory can properly explain integrated untensities for real crystals with strong primary extinction.

It is our purpose to prove that this conclusion is based on some inadequacies in Kato's solution to (6) and (9). A correct solution, given here, reproduces the observations of Olekhnovich *et al.* rather closely.

In § II, we consider the properties of the solution to (6) and (9). Its application to the experiment of Olekhnovich *et al.* is reported in § III. (We finally discuss some general conclusions which arise from this study.)

II. Solution for a real crystal

II.1. *Boundary conditions*

The boundary conditions for the beams at the surface of the crystal are crucial.

It has been shown (Kato, 1976; Becker, 1977) that starting from a point source at various points on the surface of the crystal one can easily obtain the integrated intensities for extended sources by optical transforms from spherical to plane waves.

We therefore consider a point source at the surface, and take this point S as origin, for an incident beam of unit intensity

$$D_0 = \delta(s_h). \tag{14}$$

It follows from (6) and (9) that the effective absorption coefficients are μ_e and $\tilde{\mu}_e$ for the coherent and incoherent beams respectively. With this notation, we get

$$\begin{aligned} &\langle D_0(\varepsilon, s_h)\rangle = 0 \\ &\langle D_h(s_0, \varepsilon)\rangle = i\kappa_h E \exp(-\tfrac{1}{2}\mu_e s_0) \\ &I_0^i(\varepsilon, s_h) = 0 \\ &I_h^i(s_0, \varepsilon) = |\kappa_h|^2(1-E^2)\exp(-\tilde{\mu}_e s_0), \end{aligned} \tag{15}$$

where ε is a distance small with respect to Λ, but at least of dimension τ. In other words, $\tau/\Lambda \ll 1$, an implicit assumption of Kato's theory.

Boundary values (15) are simply the result of kinematic theory, averaged over a distance of order τ. This is why μ_0 is replaced by an effective value μ_e or $\tilde{\mu}_e$. Equations (15) are fully consistent with (6) and (9), but this result is far from being obvious.

Furthermore, we shall assume pure Laue-type geometry. Let M be the point at which a beam originating at S will exit from the crystal (Fig. 1).

We will suppose that the whole parallelogram $SmMn$ belongs to the sample. This approximation has been discussed in various circumstances (Becker & Coppens, 1974; Becker, 1977; Becker & Dunstetter, 1984): it is the only case where a general tractable solution is possible. The error this assumption introduces increases with growing scattering angle, but for most applications is reasonably small. Moreover, for a parallel plate in transmission geometry, the situation of Fig. 1 is always true and there is no error.

II.2. *Two limit cases*

II.2(a). We suppose $E = 0$, thus a complete lack of coherence.

$$\langle D_h\rangle = 0.$$

Equations (9) become

$$\begin{aligned} \partial I_0/\partial s_0 &= -[\mu_0 + 2\,\mathrm{Re}\,(\kappa^2)\tau]I_0 + 2|\kappa_{-h}|^2\tau I_h \\ \partial I_h/\partial s_h &= -[\mu_0 + 2\,\mathrm{Re}\,(\kappa^2)\tau]I_h + 2|\kappa_h|^2\tau I_0. \end{aligned} \tag{16}$$

These propagation equations are equivalent to mosaic propagation equations (Kato, 1976), and differ from the conventional equations for secondary extinction (Zachariasen, 1967; Becker & Coppens, 1974). This difference was discussed by Becker & Dunstetter (1984). In fact, the secondary-extinction theory of Kato (1976) contains the correlation length τ_2 rather than τ (see equations 5): this difference leads to one of the difficulties with the present Kato statistical formulation.

II.2(b). At the opposite limit, $E = 1$, with a perfect coherence. We retrieve perfect-crystal theory.

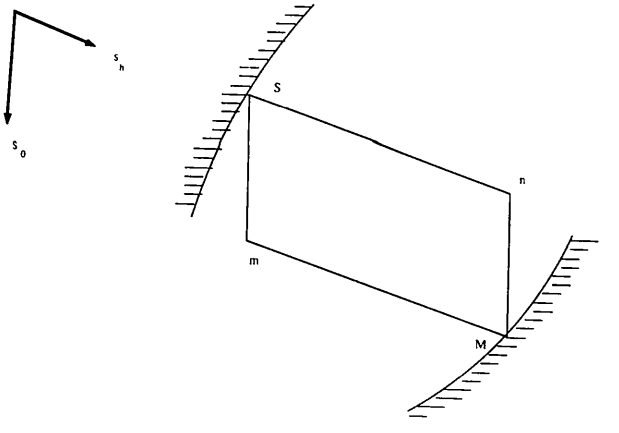

Fig. 1. Assumed simplified geometry for Bragg diffraction.

As a consequence of this discussion, we believe Kato's theory to be far more adequate for crystals with large E than small E.

II.3. *Definitions*

Let us define the quantities ψ_0, ψ_h, $\mathscr{I}_0$, $\mathscr{I}_h$, $\mathscr{I}_0^c$ and $\mathscr{I}_h^c$:

$$\begin{aligned}
\langle D_0\rangle &= \psi_0 \exp\left[-\tfrac{1}{2}\mu_e(s_0+s_h)\right]\\
\langle D_h\rangle &= \psi_h \exp\left[-\tfrac{1}{2}\mu_e(s_0+s_h)\right]\\
I_0^i &= \mathscr{I}_0^i \exp\left[-\tilde{\mu}_e(s_0+s_h)\right]\\
I_h^i &= \mathscr{I}_h^i \exp\left[-\tilde{\mu}_e(s_0+s_h)\right]\\
I_0^c &= \mathscr{I}_0^c \exp\left[-\tilde{\mu}_e(s_0+s_h)\right]\\
I_h^c &= \mathscr{I}_h^c \exp\left[-\tilde{\mu}_e(s_0+s_h)\right].
\end{aligned} \tag{17}$$

Equations (6) and (9) simplify as

$$\begin{aligned}
\partial\psi_0/\partial s_0 &= i\kappa_{-h}E\psi_h\\
\partial\psi_h/\partial s_h &= i\kappa_h E\psi_0
\end{aligned} \tag{18}$$

$$\begin{aligned}
\partial\mathscr{I}_0^i/\partial s_0 &= \tilde{\sigma}_{-h}\mathscr{I}_h^i + \sigma_{-h}(1-E^2)\mathscr{I}_h^c\\
\partial\mathscr{I}_h^i/\partial s_h &= \tilde{\sigma}_h\mathscr{I}_0^i + \sigma_h(1-E^2)\mathscr{I}_0^c.
\end{aligned} \tag{19}$$

Equations (18) are equivalent to the perfect-crystal Takagi-Taupin equations, where F_h has been replaced by (F_hE). We expect E to be a Gaussian in (hkl), inseparable from the usual temperature factor. The occurrence of this term might be related to the well known observed discrepancy between Debye-Waller factors obtained by neutron and X-ray diffraction, since E values are expected to be different for the samples used in the X-ray and neutron experiments. It seems that E could only be separated out from data analysis by varying the temperature, since, in contrast to Debye-Waller factors, it should not depend strongly on temperature.

The solution of (18) leads to

$$\begin{aligned}
I_0^c &= E^2|\kappa|^2(s_0/s_h)|J_1[2\kappa E(s_0s_h)^{1/2}]|^2\\
&\quad\times\exp\left[-\mu_e(s_0+s_h)\right]\\
I_h^c &= E^2|\kappa|^2|J_0[2\kappa E(s_0s_h)^{1/2}]|^2\\
&\quad\times\exp\left[-\mu_e(s_0+s_h)\right],
\end{aligned} \tag{20}$$

where J_0 and J_1 are Bessel functions of order 0 and 1.

II.4. *Solving equations* (19)

We now solve equations (19) with the help of propagation operators (Becker, 1977).

The solution can be written as follows: $\hat{L}$ is a linear operator (propagator) such that

$$g(s_0, s_h) = \hat{L}(f) = \tilde{\sigma}^2 \int_0^{s_0} \mathrm{d}u \int_0^{s_h} \mathrm{d}v f(u, v).$$

The action of L is to propagate the scattering events from (u, v) to (s_0, s_h).

$$\begin{aligned}
&\mathscr{I}_h^i - \tilde{\sigma}^2 \int_0^{s_0}\int_0^{s_h} \mathrm{d}u\,\mathrm{d}v\,\mathscr{I}_h^i(u, v)\\
&\quad = [1-\hat{L}]\mathscr{I}_h^i\\
&\quad = |\kappa_h|^2(1-E^2) + \tilde{\sigma}_h\sigma_{-h}(1-E^2)\int_0^{s_0}\int_0^{s_h} \mathrm{d}u\,\mathrm{d}v\,\mathscr{I}_h^c(u, v)\\
&\qquad + \sigma_h(1-E^2)\int_0^{s_h} \mathscr{I}_0^c(s_0, v)\,\mathrm{d}v\\
&\quad = f^0 + f^1 + f^2.
\end{aligned}$$

Thus,

$$\mathscr{I}_h^i = [1-\hat{L}]^{-1}(f^0+f^1+f^2) \tag{21}$$

and the solution is the sum of three terms:

$$\begin{aligned}
\mathscr{I}_h^i &= \mathscr{I}_h^0 + \mathscr{I}_h^1 + \mathscr{I}_h^2\\
\mathscr{I}_h^p &= \sum_{n=0}^{\infty} \hat{L}^n[f^p], \qquad p = 0, 1, 2.
\end{aligned} \tag{22}$$

For $\mathscr{I}^0$ (Kato, 1976, 1980*c*; Becker, 1977), one finds

$$\mathscr{I}_h^0 = |\kappa_h|^2(1-E^2)I_0[2\tilde{\sigma}(s_0s_h)^{1/2}], \tag{23a}$$

which corresponds to the neglect of coherent contribution, *i.e.* pure mosaic theory. The intensity in the incident beam at s_0, s_h is obtained as

$$\mathscr{I}_0^0 = \tilde{\sigma}/\tilde{\sigma}_h|\kappa_h|^2(1-E^2)(s_0/s_h)^{1/2}I_1[2\tilde{\sigma}(s_0s_h)^{1/2}], \tag{23b}$$

where I_0 and I_1 are modified Bessel functions.

In order to evaluate $\mathscr{I}_h^{1,2}$, we will make use of a theorem which is proved in Appendix *A*.

Theorem: Consider the equation

$$\begin{aligned}
(1-\hat{L})\mathscr{I} &= f * g\\
&= \int_0^{s_0}\int_0^{s_h} f(u, v)g(s_0-u, s_h-v)\,\mathrm{d}u\,\mathrm{d}v.
\end{aligned}$$

We get

$$\hat{L}[f*g] = \hat{L}f * g = f * \hat{L}g$$

and finally

$$\mathscr{I} = f * \left[\sum_{n=0}^{\infty} \hat{L}^n(g)\right] = \left[\sum_{n=0}^{\infty} \hat{L}^n(f)\right] * g. \tag{24}$$

We first consider f^1. We may write

$$f^1 = (\tilde{\sigma}_h\sigma_{-h}/|\kappa_h|^2)\mathscr{I}_h^c * f^0.$$

As a consequence, we immediately obtain

$$\mathscr{I}_h^1 = (\tilde{\sigma}_h\sigma_{-h}/|\kappa_h|^2)\mathscr{I}_h^c * \mathscr{I}_h^0. \tag{25}$$

Similarly for f^2:

$$f^2 = \sigma_h(1-E^2)\mathscr{I}_0^c * \delta(s_0)$$

$$\sum_{n=0}^{\infty} \hat{L}^n[\delta(s_0)] = \delta(s_0) + \tilde{\sigma}(s_h/s_0)^{1/2}I_1[2\tilde{\sigma}(s_0s_h)^{1/2}]$$

and

$$\mathcal{J}_h^2 = \sigma_h(1-E^2)\int_0^{s_h} \mathcal{J}_0^c(s_0, v)\,dv + (\sigma_h\tilde{\sigma}_h/|\kappa_h|^2)\mathcal{J}_0^c * [\mathcal{J}_0^0 s_h/s_0]. \quad (26)$$

The first term in (26) was neglected by Kato.

II.5. *The physical picture*

Let us try to find a physical picture to the solution for the incoherent intensity. It can be decomposed as

$$I_h^i = I_h^{i0} + I_h^{i1} + I_h^{i2}. \quad (27)$$

The first term I_h^{i0} corresponds to a purely incoherent propagation from the surface. This means that some phase coherence is lost in the immediate vicinity of S.

$$I_h^{i0} = |\kappa_h|^2(1-E^2)I_0[2\tilde{\sigma}(s_0 s_h)^{1/2}] \times \exp[-\tilde{\mu}_e(s_0+s_h)]. \quad (28a)$$

With a similar expression for the incident beam

$$I_0^{i0} = |\kappa_h|^2(\tilde{\sigma}/\tilde{\sigma}_h)(1-E^2)(s_0/s_h)^{1/2}I_1[2\tilde{\sigma}(s_0 s_h)^{1/2}] \times \exp[-\tilde{\mu}_e(s_0+s_h)], \quad (28b)$$

I_h^{i1} can be written as

$$I_h^{i1} = (2\sigma_{-h}\tau_e)I_h^c * I_h^{i0} \quad (29)$$

and has the following meaning (Fig. 2).

At the point (u, v), the diffracted coherent beam $I_h^c(u, v)$ is scattered into the incident direction and we assume phase coherence to be lost over a distance $2\tau_e$. At a point within a distance $2\tau_e$ from (u, v) along the incident beam, a new scattering occurs where phase coherence is lost and from that point the beam travels incoherently. I_h^{i1} is the sum of all these events for variable (u, v). Since we assume $\tau_e \ll s_0, s_h$, the quantity I_h^{i2} is expressed by

$$I_h^{i2} = \sigma_h(1-E^2)\int_0^{s_h} dv\, I_0^c(s_0, v)\exp[-\tilde{\mu}_e(s_0+v)] + [2\sigma_h\tau_e]I_0^c * [(s_h/s_0)I_0^{i0}]. \quad (30)$$

The second term in (30) corresponds to the following situation (Fig. 3). The incident coherent beam is scattered at (u, v) into the diffracted direction. We assume coherence to be lost over a distance of order $2\tau_e$. From a point within a distance $2\tau_e$ from (u, v) along the diffracted beam, the propagation is incoherent. We notice that

$$(s_h/s_0)I_0^{i0}(s_0, s_h) = I_0^{i0}(s_h, s_0),$$

which corresponds to an interchange of incident and diffracted directions. $I_0^{i0}(s_h - v, s_0 - u)$ corresponds to a diffracted beam at M originating from a unit intensity in the diffracted direction at (u, v).

The first term in (30) corresponds to the case where a coherent beam in the incident direction reaches mM, is scattered and cannot be rescattered, thus simply propagating in the diffracted direction.

We notice that $2\tau_e$ is the apparent coherence length in (29) and (30); this cannot be guessed from the Takagi-Taupin equations. It involves the parameter Γ, and this difficult part of the theory will be discussed in detail in a forthcoming paper.

II.6. *Integrated intensity-case of a parallel plate*

It has been shown (Kato, 1976; Becker, 1977) that the integrated intensity for an extended incident beam can be easily obtained from the intensity corresponding to a point source.

$I(m)$ denotes the intensity at m from a point source at S, the beam exiting at M. Remember that the pair (S, M) is unambiguously defined by the point m inside the crystal. The integrated power in the reflected beam, P, is given by

$$P = [\lambda/\sin(2\theta)]\int_v I(m)\,dv_m, \quad (31)$$

where

$$I(m) = I_h^c + I_h^i, \qquad I_h^i = I_h^{i0} + I_h^{i1} + I_h^{i2}.$$

Thus

$$P = P^c + P^i, \qquad P^i = P^{i0} + m, \quad (32)$$

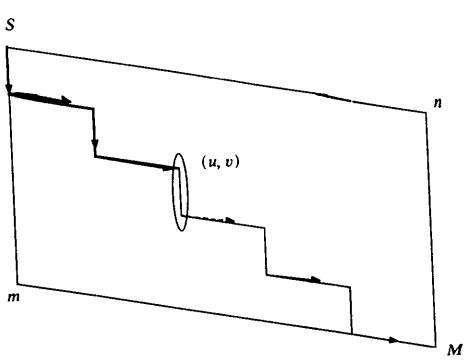

Fig. 2. Transformation of coherent diffracted into incoherent process, at point (u, v).

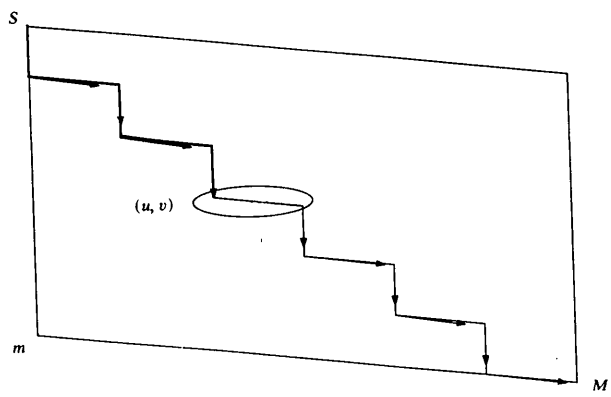

Fig. 3. Transformation of coherent incident into incoherent process, at point (u, v).

where m corresponds to the mixed components I_h^{i1} and I_h^{i2}.

The calculation of (31) is done by numerical integration for a crystal of general shape, but an analytical solution can be obtained for a parallel plate in transmission geometry.

As the detailed integration of (31) is quite similar to K*b*, it will not be repeated here. Our values for P^c and P^{i0} are equivalent to Kato's result. However, the value of m turns out to be rather different. For a parallel plate, we find

$$P^{i1} = (4/\gamma_h) M_h^{(2)}, \tag{33}$$

where $M_h^{(2)}$ is a quantity defined by Kato (K*b*, equation 19*d*) and

$$P^{i2} = (4/\gamma_0) M_h^{(1)} + P'^i. \tag{34}$$

$M_h^{(1)}$ is given in K*b*, equation (19*c*) and P'^i corresponds to a term not included by Kato. With Kato's notation,

$$P'^i = 2E^2(1-E^2)\kappa^2 \tau Q[\gamma_0(\gamma_0\gamma_h)^{1/2}]^{-1} \times \{\exp[-(\tilde{M}-\tilde{N})_t] * L_0\}_t. \tag{35}$$

Finally, in symmetrical Laue cases, the mixed power is

$$m = E(1-E^2) H_h \{\tfrac{1}{2}(m_1+m_2) - n_2\} \tag{36}$$

to be compared with K*b* equation (36*b*).

We have checked this difference by three methods: analytical integration, numerical calculation and integration by the procedure developed by Kato.

Equations (33) and (34) summarize the modifications from Kato's original solution in the case of a parallel plate. Similar modifications, to be incorporated in a solution for a crystal of general shape, will be given in a forthcoming publication.

Let us finally discuss the influence of this modification on the integrated power in the diffracted beam. In Fig. 4 various components are plotted, for a non-absorbing case, and with the conditions used by Kato [$E = 0{\cdot}9$, $\tau/\Lambda = 0{\cdot}1$], *versus* $2(T/\Lambda)$, where T is the effective crystal thickness, for a non-absorbing case.

The mixed component m is increased by a factor of 4, compared with the original value m_K (see also Fig. 3 in K*b*). The consequence is a much larger contribution of incoherence even for crystals of high long-range perfection (high E).

In Fig. 5, we give the same plot for $E = 0{\cdot}1$, $\tau/\Lambda = 0{\cdot}1$ and though the same qualitative change occurs, the effect of the mixed component remains small. The smallness of the modification for the case of $E \ll 1$ does not in fact mean that (6) and (9) in their present form are well adapted to this situation.

Thus, we expect a very delicate balance between coherent and incoherent components in the case of crystals with a high degree of perfection, *i.e.* for severe primary extinction effects.

We will discuss the case of silicon in the next section.

III. Application to silicon crystals with high degree of perfection

III.1. *Experimental and original analysis*

Olekhnovich *et al.* (1983) have measured diffracted power from various parallel plates of silicon, using Cu $K\alpha$ radiation, with samples of various dislocation densities. They worked in the symmetrical Laue geometry and varied the apparent thickness by rotating the sample around the reciprocal-lattice vector.

These authors used samples with low dislocation density: $N_d = 30\ \text{mm}^{-2}$ for sample I, $N_d = 100\ \text{mm}^{-2}$ for sample II, and also samples with high dislocation density ($N_d > 5000\ \text{mm}^{-2}$). In the present study, we shall discuss samples I and II, for which primary extinction is important.

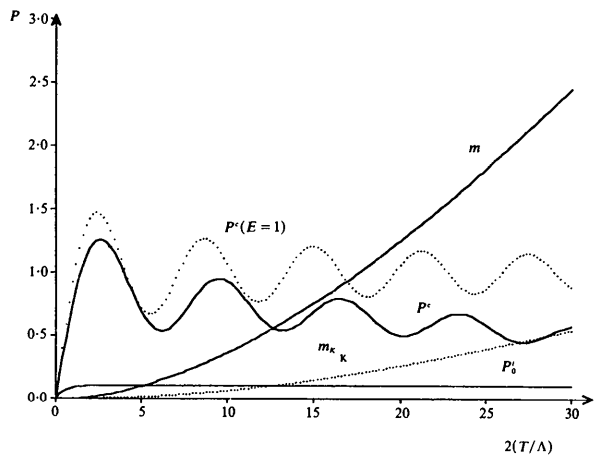

Fig. 4. Diffracted power (divided by H_h, non-absorbing case) as a function of $2(T/\Lambda)$, for $E = 0{\cdot}9$, $\tau/\Lambda = 0{\cdot}1$.

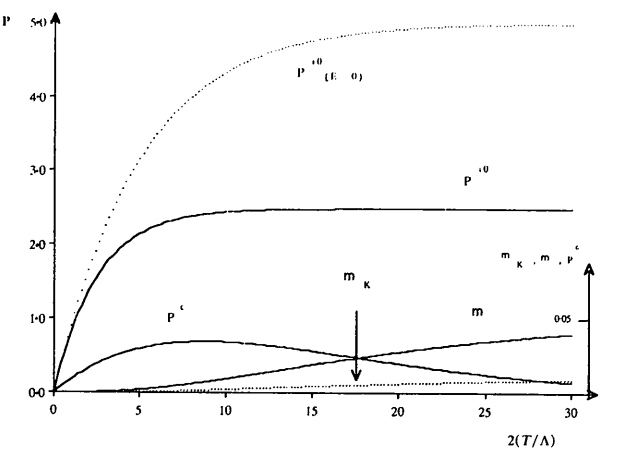

Fig. 5. Diffracted power (divided by H for non-absorbing case) as a function of $2(T/\Lambda)$, for $E = 0{\cdot}1$, $\tau/\Lambda = 0{\cdot}1$.

If t is the effective thickness of the plate in the plane defined by the incident and diffracted beams, the optical length is $T = t/\cos\theta$.

For sample II, Olekhnovich *et al.* results for the 333 reflection are shown in Fig. 6, where the 'reduced intensity' is plotted *versus* $A = T/\Lambda$. Curve (1) corresponds to experimental points, and curve (2) to the best agreement with Kato's theory. The 'reduced theoretical intensity' is defined as

$$R_{r\,\mathrm{th}} = 2A(P_{\mathrm{th}}/P_k), \qquad (37)$$

where P_k is the kinematical diffracted power and P_{th} is the theoretical diffracted power as defined in (31). This definition of R_{th} is such that $R_{\mathrm{th}} \to 1$ for a large perfect crystal (dynamical limit). $R_{r\,\mathrm{th}}$ corresponds to curve (2). Absorption, anomalous Bormann absorption and anomalous scattering play a significant role in this study.

Because of the smallness of incoherent and mixed components in Kato's expression, Olekhnovich *et al.* assumed that only the coherent component is affected by anomalous scattering and absorption: they corrected for it using a method proposed by Kato (1968). As a consequence, the experimental points on curve (1) of Fig. 6 correspond to

$$R_{r\,\mathrm{exp}} = (2A/P_k)[P_{\mathrm{exp}} - P_{\mathrm{an}}], \qquad (38)$$

where P_{exp} is the experimental power and P_{an} is the calculated correction for the anomalous effect in the coherent part.

We observe that oscillations are highly visible, attesting the high E value. In fact, the best fit was found by Olekhnovich *et al.* for $E \sim 0{\cdot}97$ and $\tau/\Lambda \sim 0{\cdot}20$. We can estimate the accuracy of the fit by

$$\eta = \frac{1}{N}\sum_k \frac{|R_{r\,\mathrm{th}} - R_{r\,\mathrm{exp}}|}{R_{r\,\mathrm{exp}}},$$

in which N is the number of experimental points. Olekhnovich *et al.*'s study leads to $\eta \sim 25\%$. Kato's original theory strongly underestimates reduced intensities, in particular for large values of A. The strong deviation of R from 1 for large A shows that even slight distortions rapidly destroy coherence. Olekhnovich *et al.* also varied Γ in the definition of τ_e (equations 11 and 12) but this leads only to a very small improvement.

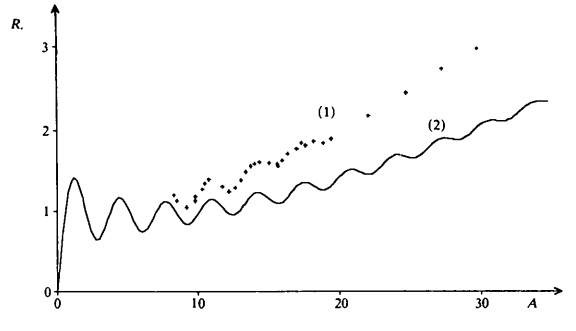

Fig. 6. Reduced intensity for the 333 reflection of Si, as a function of A. Curve (1) experimental points; curve (2) best fit from Kato's theory. (From Olekhnovich *et al.*, 1983.)

III.2. *Modified analysis*

We reconsidered this analysis with the modifications in § II of this paper. A proper integration of propagation equations leads to a strong increase of the mixed component for large A, even in the case of high E values. One can no longer neglect anomalous effects in the mixed component.

Thus, we directly introduce anomalous dispersion in the equations for the diffracted power replacing the atomic scattering factor f_0 by $f = f_0 + \delta f' + i\delta f''$. $\delta f'$ and $\delta f''$ are taken respectively as 0·244 and 0·33 (*International Tables for X-ray Crystallography*, 1974).

Fig. 7 shows the influence of anomalous scattering on the 333 reflection intensity. This example corresponds to $E = 0{\cdot}97$ and $\tau/\Lambda = 0{\cdot}20$. In curve (1), the Borrmann effect is totally neglected ($f = f_0$). In curve (2), only the coherent component is corrected for the Borrmann effect, while curve (3) corresponds to the correct calculation, where all components include anomalous contributions. The effect is very significant for large values of A.

Fig. 8 shows our results for the 333 reflection and sample II. As experimental values we take $y = P_{\mathrm{exp}}/P_k$ measured by Olekhnovich *et al.* (Fig. 2 from Olekhnovich *et al.*, 1983). In Fig. 8, we plot $Y = 2Ay$ as a function of A. Curve (1) represents the experimental points. Curve (2) corresponds to the least-squares fit that led to $E = 0{\cdot}91$ and $\tau/\Lambda = 0{\cdot}0134$. The agreement factor η is now 7·8%. A variation of Γ even leads to $\eta \sim 6{\cdot}7\%$. We observe a very significant improvement if we compare this with Fig. 6.

In Fig. 9 we present similar results for sample I. The optimization leads to $E = 0{\cdot}95$ and $\tau/\Lambda = 0{\cdot}011$. η is 4·7% and reduces to 4% if Γ is varied.

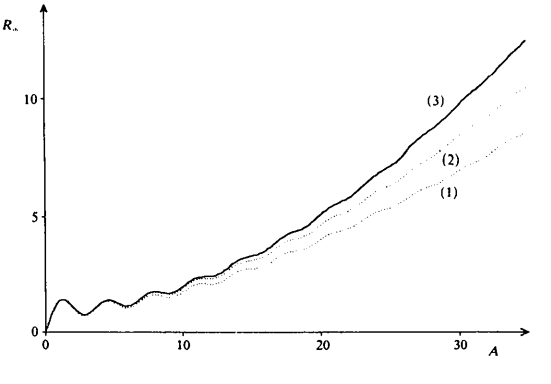

Fig. 7. Influence of anomalous scattering on the reduced intensity, for $E = 0{\cdot}97$, $\tau/\Lambda = 0{\cdot}20$. Curve (1) neglect of Borrmann effect; curve (2) Borrmann effect only in the coherent component; curve (3) complete calculation.

III.3. *Conclusions*

We conclude that Kato's theory is well adapted to crystals of high long-range-order perfection. One can well reproduce the oscillations for small A as well as the observed increase of the intensity for large A.

Anomalous scattering can be included in the theory. The importance of mixed components to the diffracted intensity is clearly demonstrated. Moreover, for cases of low dislocation density, it would be incorrect to consider that extinction is only of primary type. For instance, curve (3) of Figs. 8 and 9 shows the behaviour of a pure primary-extinction correction: both the pseudoperiod of the oscillations and the average slope are wrong: the agreement factor η would be 17% for sample II and 11% for sample I.

IV. Concluding remarks

IV.1. *Kato's approach*

We have seen that Kato's approach fills the gap between pure dynamical theory and 'secondary-extinction theory'. For crystals with a very low dislocation density, one cannot apply pure dynamical theory. 'Mixed terms' which represent the occurrence of incoherence somewhere in the bulk of the sample have to be taken into account, in additional to the purely coherent and purely incoherent components.

The influence of the anomalous-scattering effect is very important.

Our first conclusion is that, with a careful solution of Kato's statistical propagation equations, extinction effects for highly perfect crystals can be reproduced. Experience with other examples is needed. The integration of (6) and (9) has been performed for crystals of general convex shape and this will be the object of a forthcoming publication, where the solution will be given in terms of a programmable expression where the parameters for a least-squarès routine are E and τ (in fact their h, k, l dependence).

IV.2. *Problems with new formulation*

However, there are some difficulties with the present formulation of (6) and (9); and especially with the incoherent part of the intensity. We recast the effective correlation length as

$$\tau_e = (1-E^2)\tau + E^2\Gamma, \tag{39}$$

where Γ is the correlation length of the incoherent part of the beams. Obviously, Γ is not independent of τ and Λ. Kato discusses this point and proposes that $\Gamma = \Lambda/E$, which leads to

$$\tau_e = (1-E^2)\tau + E\Lambda. \tag{40}$$

If the crystal is composed of completely randomly distributed perfect blocks ($E \neq 0$ and $\tau \to 0$), Takagi-Taupin equations can be directly solved, leading to

$$I_h = |\kappa_h|^2\{E^2|J_0[2\kappa E(s_0 s_h)^{1/2}]|^2 + (1-E^2)\}.$$

Integration of (9) would lead to this result only if $\tau_e \to 0$, which means $\Gamma \to 0$, in contradiction with (40).

The only way to improve the theory is to make an assumption concerning the shape of the correlation function $g(z)$ and to try to derive a plausible expression for τ_e and the propagation equation for the incoherent part of the beam: see for instance Kulda (1984).

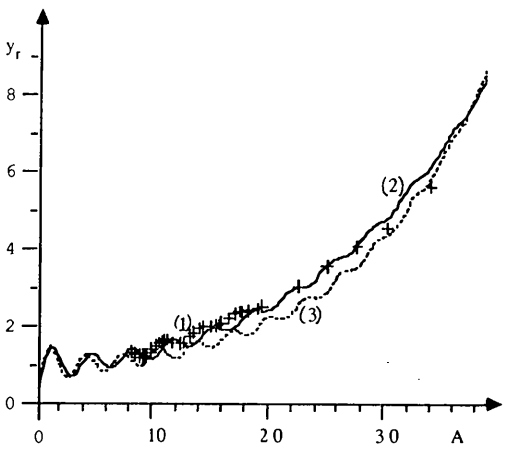

Fig. 8. Reduced extinction y as a function of A, for sample II. Curve (1) experimental points (+); curve (2) best least-squares fit (——); curve (3) primary extinction (------).

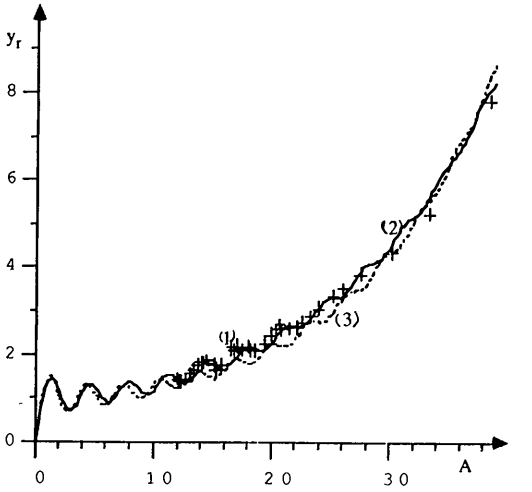

Fig. 9. Reduced extinction y as a function of A, for sample I. Curve (1) experimental points (+); curve (2) best least-squares fit (——); curve (3) primary extinction (------).

We thank Professor Philip Coppens for very helpful discussions and a critical reading of this paper.

APPENDIX A

We want to prove that

$$\hat{L}[f * g] = [\hat{L}f] * g = f * [\hat{L}g].$$

Let

$$h(x, y) = f * g = \int_0^x du \int_0^y dv f(u, v) g(x-u, y-v)$$

$$\hat{L}(h) = \tilde{\sigma}^2 \int_0^x du \int_0^y dv\, h(u, v).$$

If h is expanded into its components f and g:

$$\hat{L}(h) = \tilde{\sigma}^2 \int_0^x du \int_0^u du' \int_0^y dv \int_0^v dv' f(u', v') \times g(u-u', v-v'),$$

we change variables (u, u') into $(u', \xi = u-u')$, (v, v') into $(v', \eta = v-v')$ and get

$$\hat{L}(h) = \tilde{\sigma}^2 \int_0^x du' \int_0^y dv' f(u', v') \times \int_0^{x-u'} d\xi \int_0^{y-v'} d\eta\, g(\xi, \eta)$$

$$= \int_0^x du' \int_0^y dv' f(u', v') \hat{L}g(x-u', y-v')$$

$$= f * [\hat{L}g]$$

$$= [\hat{L}f] * g.$$

References

AUTHIER, A. (1970). *Advances in Structure Research by Diffraction Methods*, pp. 1-52. Oxford: Pergamon Press.

BATTERMAN, B. W. & COLE, H. (1964). *Rev. Mod. Phys.* **36**, 681-717.

BECKER, P. (1977). *Acta Cryst.* A**33**, 667-671.

BECKER, P. J. & COPPENS, P. (1974). *Acta Cryst.* A**30**, 129-153.

BECKER, P. J. & COPPENS, P. (1975). *Acta Cryst.* A**31**, 417-425.

BECKER, P. & DUNSTETTER, F. (1984). *Acta Cryst.* A**40**, 241-251.

DARWIN, C. G. (1914). *Philos. Mag.* **27**, 315-333.

DARWIN, C. G. (1922). *Philos. Mag.* **43**, 800-824.

International Tables for X-ray Crystallography (1974). Vol. IV. Birmingham: Kynoch Press. (Present distributor D. Reidel, Dordrecht.)

KATO, N. (1968). *J. Appl. Phys.* **39**, 2225-2237.

KATO, N. (1973). *Z. Naturforsch. Teil A*, **28**, 604-609.

KATO, N. (1976). *Acta Cryst.* A**32**, 453-466.

KATO, N. (1980*a*). *Acta Cryst.* A**36**, 763-769.

KATO, N. (1980*b*). *Acta Cryst.* A**36**, 770-778.

KATO, N. (1980*c*). In *Electron and Magnetisation Densities in Molecules and Crystals*, edited by P. BECKER, pp. 237-250. New York: Plenum.

KULDA, J. (1984). *Acta Cryst.* A**40**, 120-126.

OLEKHNOVICH, N. M., KARPEI, A. L., OLEKHNOVICH, A. I. & PUZENKOVA, L. D. (1983). *Acta Cryst.* A**39**, 116-122.

TAKAGI, S. (1969). *J. Phys. Soc. Jpn*, **26**, 1239-1253.

ZACHARIASEN, W. H. (1945). *Theory of X-ray Diffraction in Crystals.* New York: John Wiley.

ZACHARIASEN, W. H. (1967). *Acta Cryst.* **23**, 558-564.

Acta Cryst. (1988). A**44**, 270-282

The Use of Molecular-Replacement Phases for the Refinement of the Human Rhinovirus 14 Structure

BY EDWARD ARNOLD* AND MICHAEL G. ROSSMANN

Department of Biological Sciences, Purdue University, West Lafayette, Indiana 47907, *USA*

(*Received* 8 *July* 1987; *accepted* 25 *November* 1987)

Abstract

The structure of human rhinovirus 14 has been refined, by the method of restrained least squares, to an R factor of 0·16 for various random samples between 6 and 3 Å resolution with $F > 3\sigma(F)$. As a first step the non-crystallographic symmetry parameters were optimized using the initial atomic model in a rigid-body refinement procedure. Phase determination by the molecular-replacement phase extension and refinement procedure was continued to 2·94 Å resolution, employing the improved non-crystallographic symmetry operators. The resultant structure-factor phases and weights, together with the measured amplitudes, constituted the X-ray observations used in the restrained refinement. The Hendrickson-Konnert program system [Konnert & Hendrickson (1980). *Acta Cryst.* A**36**, 344-350] was modified to incorporate non-crystallographic symmetry constraints and structure-factor phases as observations.

* Present address: Center for Advanced Biotechnology and Medicine (CABM) and Department of Chemistry, Rutgers University, Piscataway, New Jersey 08855-0759, USA.

0108-7673/88/030270-13$03.00